JOURNAL OF AGRICULTURAL AND FOOD CHEMISTRY

Article

pubs.acs.org/JAFC

Design and Characterization of Controlled-Release Edible Packaging Films Prepared with Synergistic Whey-Protein Polysaccharide Complexes

Fei Liu,[†] Yanfeng Jiang,[†] Bingjian Du, Zhi Chai, Tong Jiao, Chunyue Zhang, Fazheng Ren, and Xiaojing Leng*

CAU & ACC Joint Laboratory of Space Food; Key Laboratory of Functional Dairy Science of Beijing and Ministry of Education; College of Food Science & Nutritional Engineering; The National Dairy Industry Technology System−Beijing Innovation Team (NDITS−BIT); Beijing Higher Institution Engineering Research Center of Animal Product; China Agricultural University; No.17 Qinghua East Road, Haidian, Beijing 100083, China

Supporting Information

ABSTRACT: This paper describes an investigation into the properties of a doubly emulsified film incorporated with protein-polysaccharide microcapsules, which serves as a multifunctional food packaging film prepared using common edible materials in place of petroleum-−based plastics. The relationships between the microstructural properties and controlled release features of a series of water-in-oil-in-water (W/O/W) microcapsulated edible films prepared in thermodynamically incompatible conditions were analyzed. The hydrophilic riboflavin (V_{B2}) nano−droplets (13−50 nm) dispersed in α−tocopherol (V_E) oil phase were embedded in whey protein-polysaccharide (WPs) microcapsules with a shell thickness of 20−56 nm. These microcapsules were then integrated in 103 μm thick WPs films. Different polysaccharides, including gum arabic (GA), low-methoxyl pectin (LMP), and κ-carrageenan (KCG), exhibited different in vitro synergistic effects on the ability of both films to effect enteric controlled release of both vitamins. GA, which showed a strong emulsifying ability, also showed better control of V_E than other polysaccharides, and the highly charged KCG showed better control of V_{B2} than GA did.

KEYWORDS: *double emulsion, microencapsulation, edible film, synergistic effect, controlled release*

1. INTRODUCTION

Due to environmental laws, resource utilization, and health requirements, a great deal of attention has recently been paid to research into replacing petroleum-based plastic films with safe, biodegradable, biocompatible materials, most of which are within the pharmaceutical and food packing industries. Edible biopolymers such as starch, cellulose derivatives, chitosan, alginate, whey protein isolated, soy protein, wheat gluten, and sodium caseinate, are considered promising candidates for this purpose.[1−3] Even biocompatible and low toxic plasticizers can be used to replace conventional plasticizers, such as phthalates and other synthetic plasticizers. These are used to adjust the flexibility of film and have been studied by many research teams.[4] Nanotechnology plays an important role in improving the systems, affecting such characteristics as cytotoxicity, water vapor barriers, and mechanical properties based upon the reactions at the molecular level.[5−8]

Multifunctional edible film can not only be used for coating or packaging but also as two-dimensional delivery systems, which are able to release drugs in a controlled, systematic manner upon contact with target surfaces. There are original reports and reviews discussing how to integrate functional additives, including mineral, probiotics, vitamins, and other active matter into these films using simple mixing and double emulsion technologies.[9−13] The active biopolymers could be incorporated into the inner droplets of W/O/W emulsions, and the emulsifying biopolymers could be used to stabilize the outer droplets of emulsions. Some food-grade blends of biopolymers have been used to stabilize the emulsions and for use as nutrient carriers and antiradical films.[14] The combination of the doubly emulsified system and film system may greatly improve the film functionalities. However, related research is still cursory outside of limited rheological discussion.[15] The integration of a doubly emulsified system into film would require at least four critical factors: (1) selection of an appropriate edible biopolymer to form the desired film; (2) design of a well-functioning drug-loading double emulsion microparticle; (3) adjustment of the compatibility of the double emulsion microparticles within the film matrix; (4) triggering of the synergistically controlled release of different drugs.[16]

Although toxicity is often associated with synthetic polymers, it is undeniable that these synthetic polymers have been more developed than natural ones because they can be modified to give a wider range of properties. This is why the reports of using common food-grade materials to prepare multifunctional edible film were so pitiful (Supporting Information (SI) Figure S1). Do common food-grade materials have no potential to prepare multifunctional and controllable edible film? In this work, a doubly emulsified film was prepared using the liposoluble vitamin E (V_E) and water-soluble riboflavin (V_{B2}). V_E and V_{B2} have a long history of use in model drugs[17,18] and

Received: March 4, 2013
Revised: May 25, 2013
Accepted: May 29, 2013
Published: May 29, 2013

ACS Publications © 2013 American Chemical Society

common food-grade biopolymers, in which they are combined with such substances as whey protein, gum arabic, pectin, and carrageenan. Whey protein was selected because of its emulsification and nutrition double values, and its general application in the field of edible films.[19] For comparison purposes, the polysaccharides were selected according to their surface charges and emulsification ability. The concerned physicochemical properties of these materials were confirmed in the main text. The film-forming mechanism and the synergistic effects of the protein−polysaccharide complexes on the controlled release of the drugs were the focus of this work.

2. MATERIALS AND METHODS

2.1. Materials. Whey protein isolates (WPI, 97% w/w protein; β-lactoglobulin 85%; α-lactalbumin 10%; BSA 5%; sodium 0.5%; calcium 0.1%) were purchased from Davisco Foods International (Eden Prairie, MNA). Riboflavin (V_{B2}), α-tocopherol (V_E), pepsin (1:60 000; from crystallized and lyophilized porcine stomach mucosa), pancreatin 8× (from hog pancreas), fluorescent dye fluorescein isothiocyanate (FITC), and Nile red were purchased from Sigma Chemical Co. (St. Louis, MO). Gum Arabic (GA), low methoxyl pectin (LMP), κ-carrageenan (KCG) and soy oil were food-grade and provided by a local supplier. Polyglycerol polyricinoleate 90 (PGPR) was provided by Danisco (Suzhou, China). NaOH, HCl, K_2HPO_4, KH_2PO_4, glycerin, and *n*-hexane were analytical grades (Beijing Chemical Factory, Beijing, China).

2.2. Preparation of the Polysaccharide Solutions. Polysaccharides powder (GA, LMP and KCG) was dissolved at the concentration of 0.1, 0.2, 0.3, 0.4, 0.5% (w/w) in deionized water, respectively, and stirred for about 20 min at 50 °C in order to ensure a complete dissolution. Then the polysaccharide solutions were adjusted to pH 1.2 and 7.4 using 1 N HCl and 1 N NaOH, respectively. These solutions were used for the analysis of the pure polysaccharides.

2.3. Preparation of the WPI−Polysaccharide Solutions. The WPI powder was dissolved at 8 and 10% (w/w) in deionized water, respectively, and stirred for about 2 h and stored overnight at 4 °C to be completely hydrated. The protein was denatured in water bath at 80 °C for 30 min in order to obtain polymer form.[20] The solution was cooled at room temperature for 2 h. The polysaccharide powders were dissolved at the concentration of 0.5, 1.0, 1.5, 2.0, 2.5% (w/w) in deionized water, respectively, by stirring for about 20 min at 50 °C. The WPI−polysaccharide mixtures were prepared by combining the WPI solution with the investigated polysaccharide solution directly at WPI−polysaccharide (WPs) ratios from 8:0 to 8:0.5. The mixtures were stirred simultaneously at room temperature. The pH of the mixtures was adjusted to 8.0 using 1 N HCl and 1 N NaOH.

2.4. Preparation of the Double Emulsions. The microstructure of the double emulsion droplets are as $W_1/O/W_2$, where W_1 refers to the inner water phase, O to the oil phase, and W_2 to the outer water phase. A primary W_1/O emulsion was formed by drop-wise addition by a Pasteur pipet of 30 g V_{B2} aqueous phase (0.5 mg/mL) into the 70 g oil phase containing V_E (10% w/w) and PGPR (8% w/w). W_1/O emulsion was pre-emulsified with an Ultra Turrax homogenizer at 10 000 rpm for 10 min (Ultra Turrax, model FA25, Fluko, Germany), then passed through a nano homogenize machine (AH100D; ATS Engineering Inc., Brampton, Canada) at 500 bar for 5 min.[21] The glycerin (0.5 g/g protein) was added first into the W_2 (WPI−polysaccharide mixtures) at pH 8, and then the primary W_1/O emulsion (3 g) was added into the W_2 solution (97 g). The obtained double emulsion was pre-emulsified with an Ultra Turrax homogenizer at 10 000 rpm for 10 min, then passed through a nano homogenize machine at 100 bar for 5 min.

2.5. Zeta Potential and Particle Size. The measurements of zeta potential and particle size of the pure polysaccharide solutions, the WPs solutions and the double emulsions were carried out with a Delsa-Nano particle analyzer (Beckman Coulter, Inc.: Fullerton, CA). The refractive index of the medium (water) was 1.333 and the temperature was 25 °C.

2.6. Hydrophilic-Lipophilic Balance (HLB) Value of the Polysaccharides. The HLB values of the polysaccharides were determined using a water titration method.[22] The calibration curve was established using three different standard surfactants including Tween 20, Tween 80 and Span 20. The values of their HLB were obtained by titrating 0.5 g surfactants with water in a 20 mL isopropanol and methylbenzene mixed (isopropanol: methylbenzene = 100:15) solvent until slightly opaque, and obtained $HLB_{Tween20}$ = 16.7, $HLB_{Tween80}$ = 15, and HLB_{Span20} = 8.6.

2.7. Fourier Transform Infrared Spectroscopy (FT-IR). All spectra were obtained using a spectrometer GX FT-IR with a DTGS detector (Perkin-Elmer, Fremont, CA) infrared spectrophotometer over a range of 4000−400 cm^{-1} with a resolution of 4 cm^{-1}.

2.8. Preparation of the Double Emulsion Films. Each double emulsion solution of 5 g was poured on Plexiglas plates (8.0 × 8.0 cm) and the obtained films were dried at 22 ± 3 °C and 56 ± 8% relative humidity in a Constant Temperature and Humidity Chamber (Ningbo Southeast Instrument Co., Zhejiang, China) for at least 48 h before subsequently peeled from the casting surface for the analysis.[23]

2.9. Encapsulation Efficiencies (EEs) of the Microparticle and Films. The $W_1/O/W_2$ double emulsions were frozen at −80 °C for <12 h and freeze-dried for 48 h. For the measurement of EE of V_E (EEV_E) of the microcapsules, 50.0 ± 0.5 mg of the freeze-dried microparticles were weighed and dispersed in 5 mL of 0.5% (w/v) Tween 80 solutions. The V_E washed into the Tween 80 was extracted with hexane. The amount of the extracted V_E was determined by UV absorbance at 285 nm using a standard curve (UVmini-1240 spectrophotometer; Shimadzu, Japan; Song et al. 2009[17]), as shown in the following equation:

$$\mathrm{EE}(\%) = \frac{M_0 - M_1}{M_0} \times 100 \quad (1)$$

where M_1 is the amount of V_E extracted from the Tween 80 and M_0 is the actual amount of V_E initially added.

For the measurement of EE of V_{B2} (EEV_{B2}), 50.0 ± 0.5 mg of the freeze-dried microparticles were weighed and dispersed in 5 mL deionized water under agitation, and the dispersion was centrifuged at 8000 rpm for 5 min. The clear liquid in the middle part was collected, and the remaining oil was extracted with hexane. V_{B2} concentration in the liquid was determined by the absorbance at 445 nm with a UV-visible spectrophotometer:

$$\mathrm{EE}(\%) = \frac{W_0 - W_1}{W_0} \times 100 \quad (2)$$

dx.doi.org/10.1021/jf4009923 | J. Agric. Food Chem. 2013, 61, 5824−5833

where W_1 is the amount of V_{B2} in the clear liquid and W_0 is the actual amount of V_{B2} initially added.

For EEV_E of the film, the surface of film was washed by 50 mL of 0.5% (w/v) Tween 80 solutions. The V_E washed into the Tween 80 was measured using the method described above. For EEV_{B2} of the film, the surface of film was washed by 50 mL deionized water. The subsequent procedure was same as that of the microcapsules.

2.10. Film Thickness. Film thickness was measured using a Digital micrometer (Cheng-Du-Cheng-Liang Co., China) at 10n random positions around the film by slowly reducing the micrometer gap until the first indication of contact. Triplicate measurements were conducted for each type of the film, and the average was taken as result.

2.11. Mechanical Properties. The measurements were carried out using a load cell of 10 kg and the analysis was performed using software provided with the texture analyzer (Texture Lab Pro Version 1.13-002, Food Technology Corporation, VA). The sample films were cut into strips with 6 mm wide. The ends of the strips were mounted between cardboard grips using double-sided adhesive tape; the exposed film area was 40 × 6 mm. Initial grip separation was set to 60 mm, whereas crosshead speed was set to 1 mm/s. Tensile strength (TS, MPa) was calculated as follows:

$$\mathrm{TS} = \frac{F_t}{L \times W} \tag{3}$$

where F_t is the max stretching strength, L the length (40 mm), and W the width (6 mm). Elongation (E, %) was

$$E(\%) = \frac{\Delta L}{L_0} \times 100\% \tag{4}$$

where L_0 is the initial length of the film samples before being stretched (40 mm), ΔL stretched length when the films were break. Triplicate measurements were conducted for each type of the film, and the average was taken as result.

2.13. Water Vapor Permeability Measurements. The water vapor transmission rate (WVTR) of the films was measured using a Mocon Aquatran (model 1/50 G, Mocon Co. MN) equipped with a coulometric phosphorus pentoxide sensor (Aquatrace). The relative humidity of the dry side was 10% and that of the other side was 40%. The measurements were performed at 23 °C. The water vapor permeability (WVP) was calculated as follows:[24]

$$\mathrm{WVP} = \frac{\mathrm{WVTR} \times L}{\Delta P} \tag{5}$$

where $WVTR$ was the measured water vapor transmission rate ($g/m^2 \cdot s$) through a film, L was the mean film thickness (m), ΔP was the partial water vapor pressure difference (Pa) across the two sides of the film. Triplicate measurements were conducted for each type of the film, and the average was taken as result.

2.14. Scanning Electron Microscopy (SEM) and Transmission Electron Microscopy (TEM). SEM: The films were dried in vacuum before measurement. The samples were mounted on aluminum stubs using gum paste and covered by gold paint. The surface morphology and the cross section of the films were examined by means of scanning electron microscopy (Hitachi S-4500, Japan). All samples were examined using an accelerating beam at a voltage of 5 kV.

TEM: Double emulsions samples were prior to be placed on carbon-coated copper grids and the excess solution was removed with filter paper. The sample was dried in air for 30 min, then stained using 2% uranyl acetate for 30 min. The measurements were performed using a Hitachi S-5500 scanning electron microscope at 30 kV.

2.15. Confocal Laser Scanning Microscopy (CLSM). Double emulsions were stained with Nile red for lipid and FITC for protein and polysaccharides. A confocal laser scanning microscope (CLSM, model EZ-C1, Nikon, Japan) equipped with an Ar-ion laser (488 nm) and an He-Ne laser (543 nm) excitation sources was used to perform the measurements.[25]

2.16. In Vitro Release of V_E and V_{B2} from Films. The release rate of V_E and V_{B2} was determined by incubating in sealed tubes. One hundred mg of the film was put in 100 mL of the release media, at a stirring speed of 100 rpm and temperature of 37.0 °C. Four release media were used: (1) HCl solution (pH 1.2); (2) simulated gastric condition (pH 1.2) with 0.1% (w/v) pepsin; (3) phosphate-buffered saline (pH 7.4); and (4) simulated intestinal condition (pH 7.4) with 1.0% (w/v) pancreatin. The tubes containing the different release media were withdrawn at either 0.5 or 1 h intervals.[18] The release rate of V_E or V_{B2} was detected by UV absorbance at 288 or 445 nm using a standard curve (UVmini-1240 spectrophotometer; Shimadzu, Japan[17]), as shown in the following equation:

$$R(\%) = \frac{G_1}{G_0} \times 100 \tag{6}$$

where G_1 is the released amount of V_E or V_{B2} in the media and G_0 the actual amount of V_E or V_{B2} initially added.

2.17. Diffusion Model Analysis. The diffusion of compounds in polymeric network microstructure is generally governed by two main simultaneous events: a Brownian motion described by means of the Fick's second law and a polymer relaxation driven by stress dissipation provoked by penetrant. The latter can be described using a first order kinetic equation. A combined model of the above mechanisms was proposed in the work of Flores et al:[26]

$$\frac{M_t}{M^{eq}} = X \cdot \left\{ 1 - \frac{8}{\pi^2} \cdot \sum_{n=0}^{\infty} \frac{1}{(2n+1)^2} \cdot \exp[-(2n+1)^2 \cdot k_F \cdot t] \right\} + (1 - X) \cdot [1 - \exp(-k_R \cdot t)] \tag{7}$$

where M_t is the total mass released from the polymeric network at time t, M^{eq} the mass released at equilibrium state, k_F the Fickian diffusion rate constant ($k_F = D \cdot (\pi^2)/(l^2)$), k_R the polymer relaxation rate constant ($k_R = (1/\tau)$), l the effective diffusion distance, τ the relaxation time associated to polymer relaxation, and X the fraction of Brownian contribution. The value of X varied between 0 and 1. For $X = 1$, the above equation refers to Brownian diffusion, whereas $X = 0$, anomalous diffusion is obtained. In the investigated conditions, eq 7 could be simplified to eq 8 using the first term of the Taylor series, because the difference between one term or more terms was minor:[27]

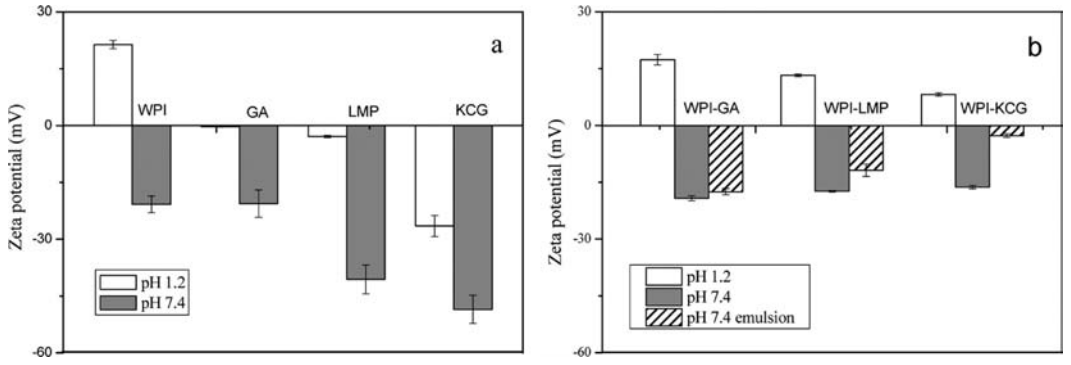

Figure 1. Zeta potential comparison of the pure components and WPs at pH 1.2 and pH 7.4. (a) Pure WPI and Ps; (b) WPs and WPsE (WPI:Ps = 8:0.5).

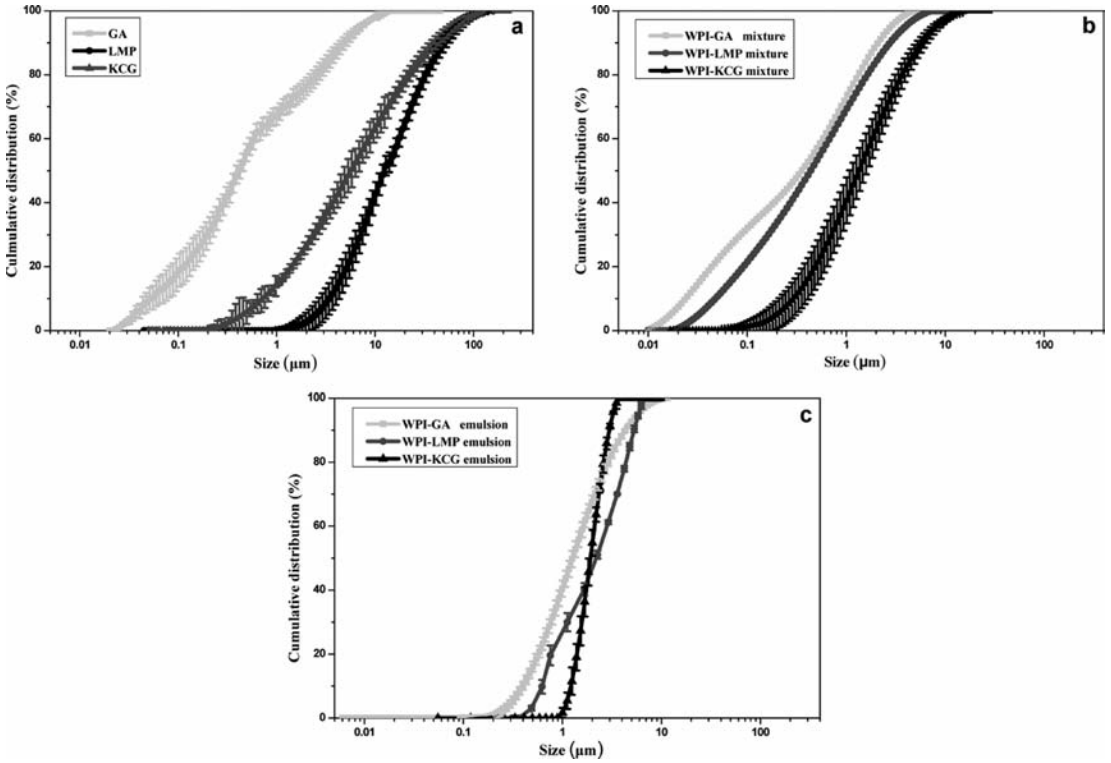

Figure 2. Cumulative size distributions of the pure (a) Ps, (b) WPs, and (c) WPsE at pH 7.4 (WPI:Ps = 8:0.5).

$$\frac{M_t}{M^{eq}} = X\cdot\left[1 - \frac{8}{\pi^2}\cdot\exp(-k_F\cdot t)\right] + (1 - X)\cdot [1 - \exp(-k_R\cdot t)] \quad (8)$$

2.18. Statistical Analyses. All experiments were performed in triplicate. Statistical data were analyzed using Origin 8.5 and SPSS 16.0. Statistics on a completely randomized design were performed using the General Linear Models procedure with the One-way analyses of variance (ANOVA). Duncan's Multiple Range Test ($P < 0.05$) was used to detect the differences among the mean values. The curve fitting was performed using a nonlinear regression analysis with the Levenberg–Marquadt algorithm for the least-squares minimization.

3. RESULTS AND DISCUSSION

3.1. Zeta Potential and Size Analysis. Figure 1 compared the zeta potential values of the pure WPI and polysaccharides (Ps) (a), the mixtures of the WPI–Ps (WPs) and the WPs film forming emulsions (WPsE) (b) at pH 1.2 and pH 7.4, respectively. The pure WPI (8%) was positively charged at pH 1.2 but negatively at pH 7.4 (the isoelectric point of WPI is about 5.2). The Ps molecules were negative and their potential values increased following the order as GA < LMP < KCG (Figure 1a) at both pH conditions. The concentration effect of the pure Ps on their potentials was minor (SI Figure S2). The potential variation of WPI by adding Ps depended on the pH medium and the type of Ps (Figure 1b and SI Figure S3). At pH 1.2, the potential decline was caused by the neutralization of the charge. In contrast, all the biopolymers were negatively charged at pH 7.4, and the system was at a thermodynamically incompatible state. This was caused by intermolecular electrostatic repulsions. In this case, a depletion effect led to an effective attraction between the protein molecules, causing protein flocculation and phase separation. There have been similar reports on the depletion effects of Ps.[28,29] This flocculation increases size, reduces mobility, and decreases

dx.doi.org/10.1021/jf4009923 | J. Agric. Food Chem. 2013, 61, 5824–5833

potential of the whole system.[23] In the WPsE systems, the potential decrease became more pronounced, indicating the formation of larger entities.

Figure 2 shows a comparison of the hydrodynamic sizes of the pure Ps, WPs, and WPsE at pH 7.4. Ps were, from smallest to largest, GA < KCG < LMP (Figure 2a), and the WPs mixtures were, from smallest to largest, WPI−GA < WPI−LMP < WPI−KCG at a WPI/Ps ratio of 8:0.5 (Figure 2b) and at lower ratios (SI Figure S4). Variations in this size of WPs were more affected by the Ps potential intensity than by Ps size. The higher the potential of the Ps, the larger the protein floc became. The order of the WPsE size variation was similar to that of the WPs, at a WPI/Ps ratio of 8:0.5 (Figure 2c) and at lower ratios (SI Figure S5).

A typical microstructure of WPs double emulsified microcapsules is shown in Figure 3. The small W_1 water droplets

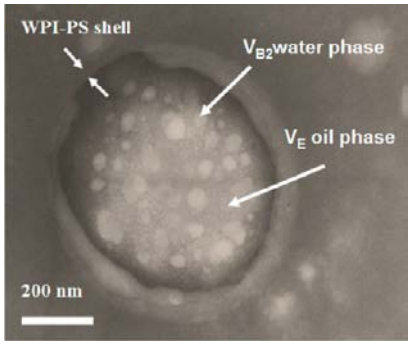

Figure 3. TEM images of typical WPI−KCG (8:0.5) double emulsified droplets.

(V_{B2} phase), whose sizes varied between 13 and 50 nm, were dispersed in V_E oil phase. The oil phase was embedded in a WPs shell. The average thickness of the WPs shell varied between 20 and 56 nm (Figure 4aa), and related to the charge and the emulsification of polysaccharide, from smallest to largest, WPI−LMP < WPI−GA ≈ WPI−KCG at a WPI/Ps ratio of 8:0.5. However, it should be denoted that the drying process of the microscopy analysis could lead to somewhat deformation of the nanoparticles. A schematic presentation of the microstructure of such double emulsified protein−polysaccharide microcapsule was shown in Figure 4ab. The shell consisted mainly of the inner protein layer, which was adsorbed directly onto the surfaces of the oil droplets, and the outer Ps layer.[30] However, unlike the microcapsule formed in acidic medium, where the protein and Ps layers were associated through electrostatic attraction, these layers maintained a certain distance between them.[21,31] This was caused by electrostatic repulsions in neutral medium.

WPs systems with different microstructures exhibited different synergistic properties with respect to drug encapsulation (Figure 5). The microcapsules' EEV_E and EEV_{B2} values increased slightly as Ps zeta potentials increased (Figure 5a and 5b), indicating that the embedding ability of the WPI shell is enhanced by depletion-flocculation at thermodynamically incompatible conditions. In contrast, only the larger, softer, and less charged Ps could raise the EE more effectively in the acidic medium.[21,31] EEV_E and EEV_{B2} of the films (Figure 5c and 5d) were significantly higher than those of the microcapsules ($P < 0.05$), indicating that the network microstructure of the films could also entrap the vitamins.

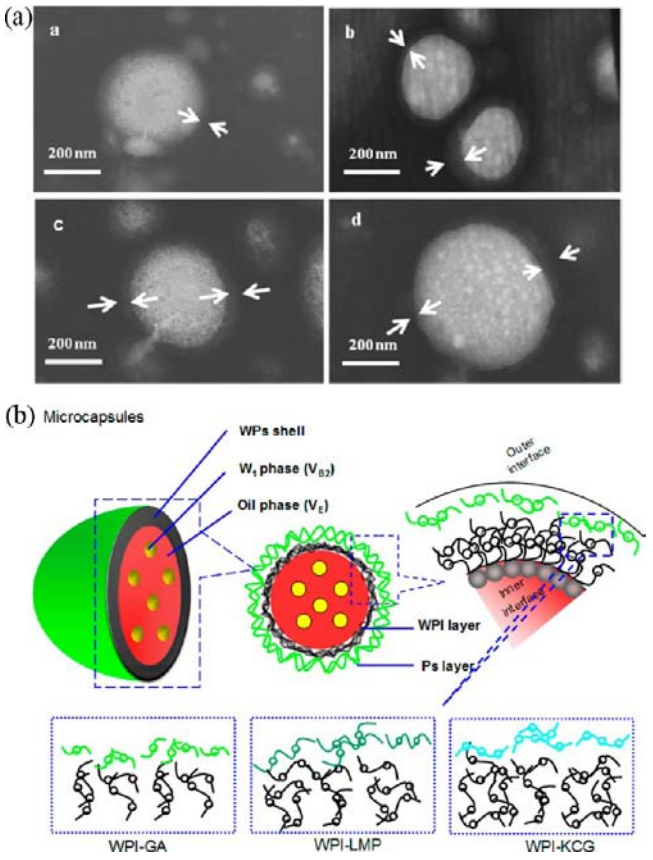

Figure 4a. (a) TEM images of the typical WPs (8:0.5) double emulsified droplets. (a) pure WPI; (b) WPI−GA; (c) WPI−LMP; (d) WPI−KCG. (b) Schematic presentation of the microstructure of the double emulsified protein−polysaccharide microcapsule.

3.2. Microstructure and Physical Properties of the Films. Figure 6 shows the microstructure and surface morphology of the films as determined by means of optical microscopy, CLSM, and SEM, respectively. With the naked eye, the surfaces of these translucent films were smooth and lacked visible pores and cracks (Figure 6a). In the CLSM photographs, the oil phase was stained red and WPs phase stained green (Figure 6b). By comparing the 8:0 and 8:0.5 films, the red color became dense with the Ps, particularly the relatively hydrophobic GA system (HLB of GA, LMP, and KCG were 8.2, 10.9, and 19.5, respectively). This indicated that the oil could be entrapped by the WPs mixed system. These observations were in accordance with the results of the encapsulation efficiency measurements. SEM cross section micrographs (Figure 6c) showed that protein flocculation could create a coarse internal microstructure. In agreement with the size analysis, the highly charged KCG and LMP were more likely to produce large aggregates in film than other polysaccharides were.

The average thickness (T) of the films was 103 ± 14 μm. Figure 7 shows a comparison of the main physical properties of packaging films,that is. the tensile strength (TS), elongation (E) and water vapor permeability (WVP) (SI Table S1). TS and E were the parameters related to the mechanical strengths of the bond matrix constituted with the biopolymer chains and WVP related to the micropaths in the film microstructure. The depletion effects permit highly charged Ps, such as LMP and KCG, to promote protein flocculation and phase separation. This renders the film microstructure discontinuous, as shown in

dx.doi.org/10.1021/jf4009923 | J. Agric. Food Chem. 2013, 61, 5824−5833

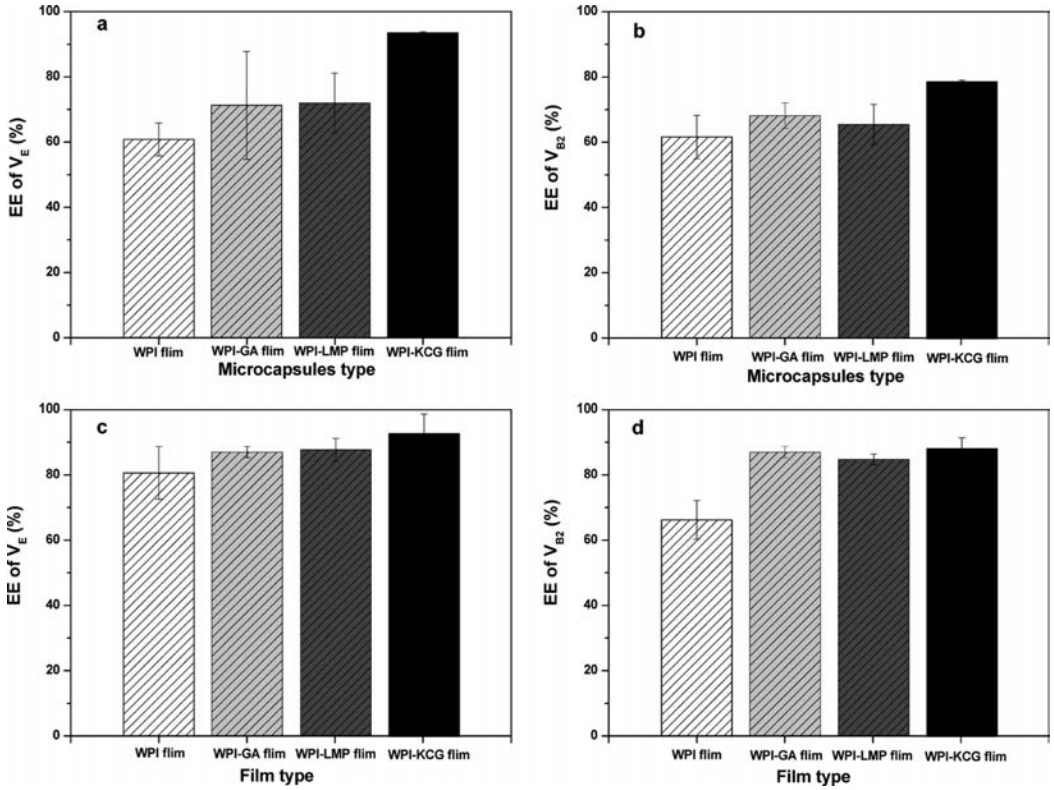

Figure 5. Comparison of the EEV_E and EEV_{B2} of the microcapsules and films. (a) EEV_E of the microcapsules; (b) EEV_{B2} of the microcapsules; (c) EEV_E of the films; (d) EEV_{B2} of the films. WPI:Ps = 8:0.5.

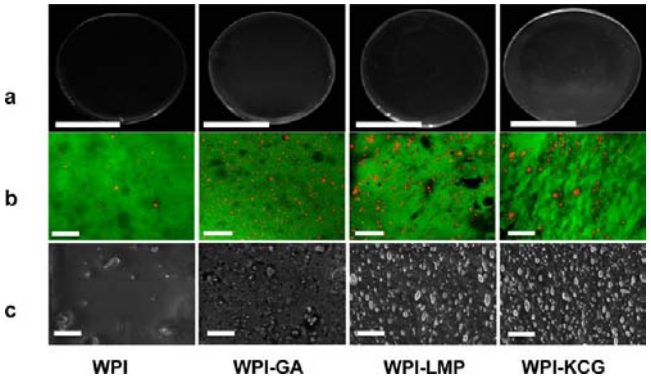

Figure 6. The microstructure and the surface morphology of the films (8:0 and 8:0.5). (a) Optical photographs; (b) CLSM micrographs of the films; (c) SEM micrographs of the film cross section. The bars were 4 cm for a, 5 μm for b and c.

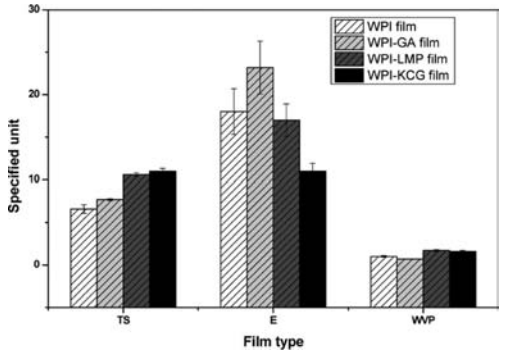

Figure 7. Comparison of the physical properties of the pure WPI and WPsE films with the mixing ratio WPI:Ps = 8:0.5. The units of TS, E, and WVP are MPa, %, and $g \cdot m \cdot m^{-2} \cdot s^{-1} \cdot Pa^{-1}$, respectively.

Figure 6. This discontinuous state led to an increase in the number and width of micropaths, which means WVP. Protein flocculation favored the reinforcement of TS and reduction of E.

3.3. Controlled Release Properties of the Films. The release rates of V_E (RV_E) and V_{B2} (RV_{B2}) of the films are shown in Figure 8 and 9, respectively. RV_E and RV_{B2} were both lower than those of the W/O/W double emulsions evaluated in our previous study.[21,31] The polymeric network structure of the film was believed to hinder the diffusion of the vitamins. This assumption was interpreted using eq 8, and the fitting results are shown in SI Tables S2 and S3.

In these tables, the values of X were generally lower at pH 1.2 and pH 7.4 without enzymes than at pH 1.2 and pH 7.4 with enzymes. Low values indicate relatively complete network microstructures within the film, and higher ones indicate damage to the microstructure from enzyme attack. The values of k_F, which is related to the Brownian behaviors of released vitamins, were roughly in the same order of magnitude regardless of the environmental pH or the presence of enzymes. For example, they were 2.0 ± 1.1 h^{-1} for V_E and 2.1 ± 0.8 h^{-1} for V_{B2}. In contrast, the change of k_R, related to the diffusion in the polymer network, was relatively large because it was affected not only by the amount of damage to the film but also by the nature of the Ps.

At pH 1.2 and pH 7.4 without enzymes, the RV_E level of the pure WPI film should be higher than those of the WPs films due to the loose structure caused by the intermolecular electrostatic repulsions. However, this phenomenon was only observed at pH 7.4 but not at pH 1.2 (Figure 8a and **c**). The

dx.doi.org/10.1021/jf4009923 | J. Agric. Food Chem. 2013, 61, 5824−5833

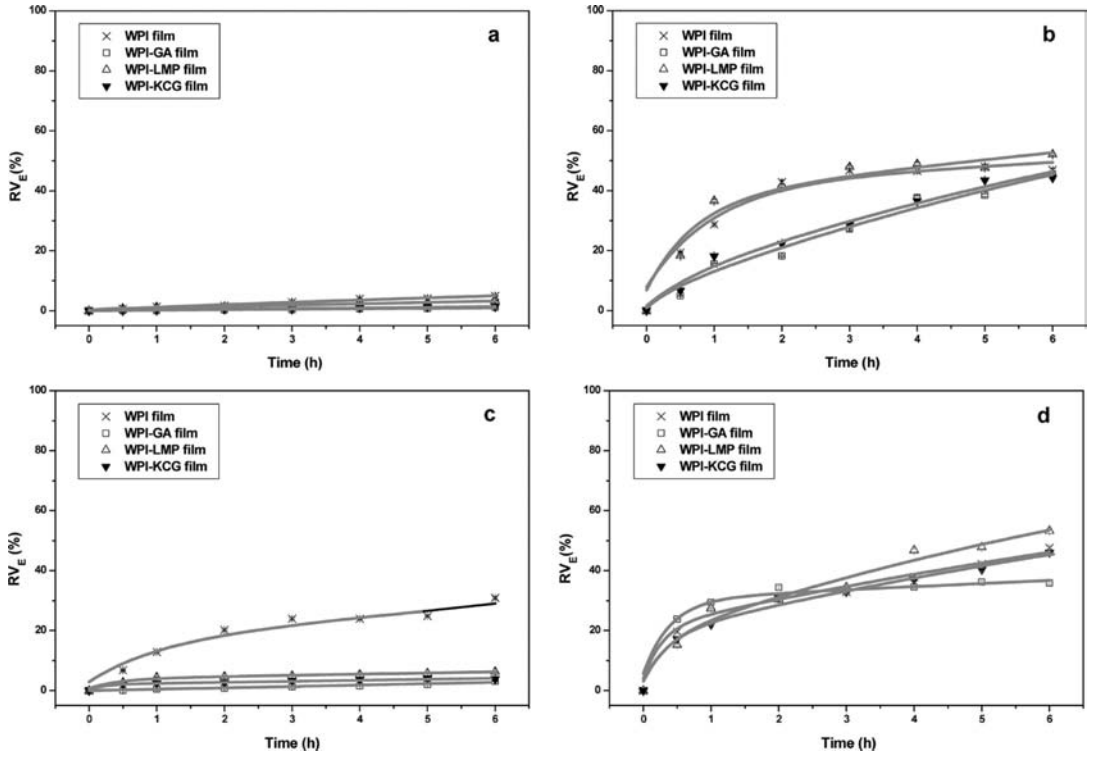

Figure 8. Comparison of the controlled RV_E of the pure WPI and WPsE films (8:0 and 8:0.5) (a) at pH 1.2 without pepsin; (b) at pH 1.2 with pepsin; (c) at pH 7.4 without pancreatin; (d) at pH 7.4 with pancreatin.

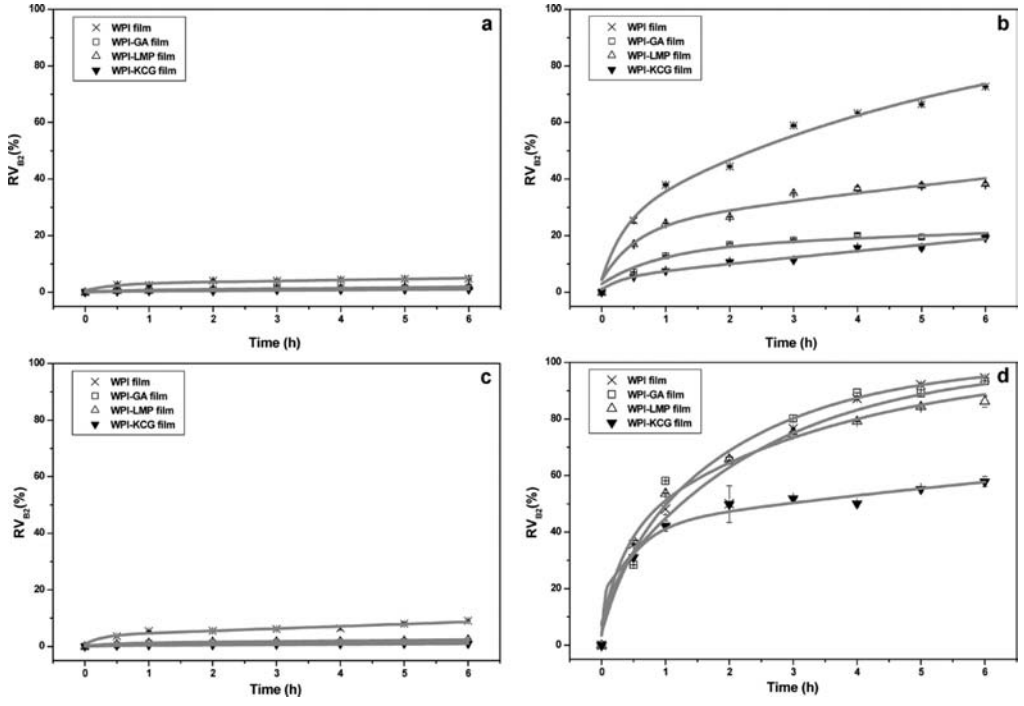

Figure 9. Comparison of the controlled RV_{B2} of the composite films to the WPI−Ps mix ratios 8:0 (pure WPI) and 8:0.5. (a) at pH 1.2 without pepsin; (b) at pH 1.2 with pepsin; (c) at pH 7.4 without pancreatin; (d) at pH 7.4 with pancreatin.

lower values of X (0.007) and k_R (0.007 h^{-1}) at pH 1.2 indicated that the release of V_E release was mainly controlled by polymer relaxation rather than Brownian mode. As mentioned in Sections 2.4 and 2.8, the film prepared at pH 8 was negatively charged. When this film was submerged in water at pH 1.2, the protein aggregated by van der Waals force as the internal pH dropped through the pI of the WPI. These aggregated protein molecules were not easily reseparated in acidic medium. This hindered the movement of V_E. Polysaccharides reinforced the protein shell through electrostatic attraction at pH 1.2 and a depletion effect at pH 7.4. Both behaviors caused declines in RV_E. GA showed the lower values

dx.doi.org/10.1021/jf4009923 | J. Agric. Food Chem. 2013, 61, 5824−5833

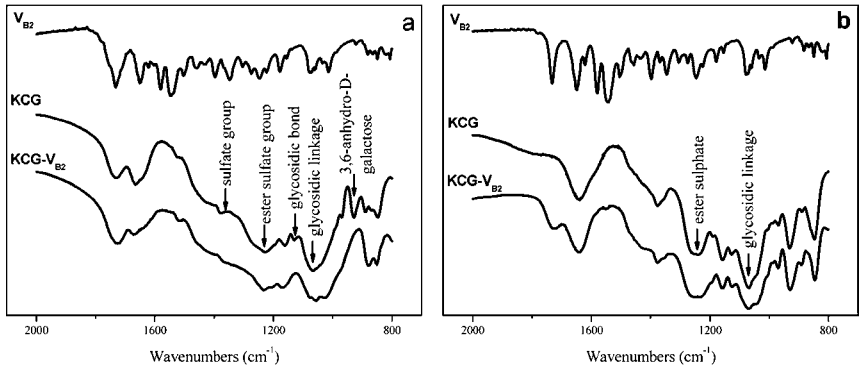

Figure 10. FTIR spectra of the V_{B2} and KCG-V_{B2} at pH 1.2 (a) and pH 7.4 (b).

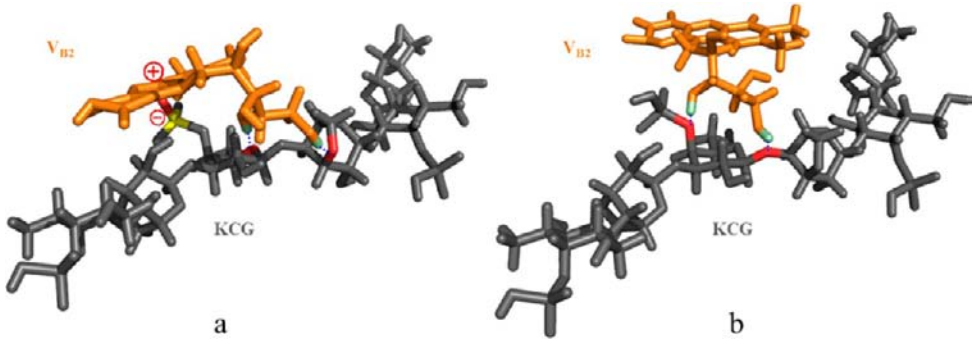

Figure 11. A proposed KCG-V_{B2} binding model at pH 1.2 (a) and pH 7.4 (b). Red, oxygen; green, hydrogen; yellow, sulfur.

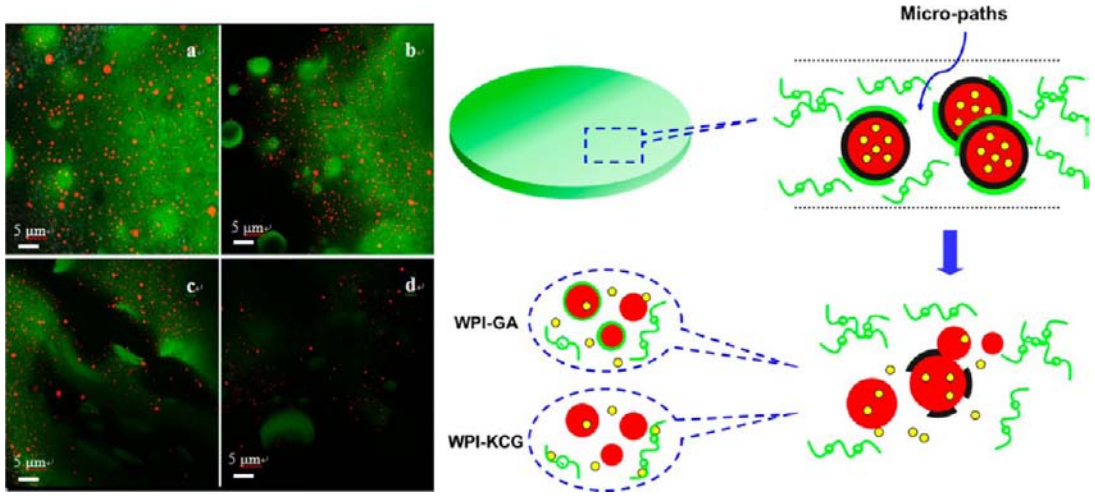

Figure 12. CLSM micrographs (left; a, 0.5 h; b, 1 h; c, 3 h; d, 6 h) and schematic presentation (right) of the degradation and controlled release process of the typical double emulsified protein−polysaccharide films. For schematic drawing, inner water phase containing VB2 was marked in yellow, oil phase in red, WPI in black and polysaccharides in green.

of X, k_R, and RV_E than other polysaccharides did. This could be attributed to its strong emulsification ability, which allowed this it to stabilize the oil in the film matrix.

At pH 1.2 and 7.4 with enzymes (Figure 8b and d), the increase in RV_E, X, and k_R indicated that the film network microstructures had been seriously damaged by enzymolysis and more V_E oil was released. At pH 1.2 with pepsin, RV_E of the WPI−GA and WPI−KCG systems were lower than those of the pure WPI and WPI−LMP systems. These phenomena are attributable to the strong emulsifying ability of GA and the relatively solid protein shell promoted by the highly charged KCG. In contrast, the difference between the RV_E of all WPsE systems, which was caused by the stronger enzymolysis of the pancreatin, was small.

As in the test of V_E, the internal pH of the film was also found to affect the amount of riboflavin released (V_{B2}) in systems lacking enzymes (Figure 9a and c). Ps maintained the ability to reinforce the protein shell and film matrix. The water-soluble molecules differ from the lipophilic molecules. Taking into account the properties of V_{B2}, a water-soluble molecule tend to be positively charged at pH 1.2 and neutral at pH 7.4.[32] In this way, the electrostatic effects between V_{B2} and the biopolymers could not be neglected. This hypothesis was verified by means of FT-IR (Figure 10). A proposed binding

dx.doi.org/10.1021/jf4009923 | J. Agric. Food Chem. 2013, 61, 5824−5833

mechanism of KCG-V_{B2} at pH 1.2 and pH 7.4 is illustrated in Figure 11.

Upon comparison of the FT-IR spectra of the pure biopolymers (WPI, GA, and LMP) and their mixtures to that of riboflavin, no modifications were found. This indicated that no complexes had formed in the WPI−V_{B2}, GA−V_{B2}, and LMP−V_{B2} system, regardless of pH (SIFigure S6). However, the KCG−V_{B2} system was different. For KCG, the region of 1380−1355 cm^{-1} was assigned to the sulfate group, the region of 1270−1230 cm^{-1} to the ester sulfate group, the peak at 1126 cm^{-1} to the asymmetric stretching of the glycosidic bond, the region from 1080−1010 cm^{-1} to the glycosidic linkage, and the region of 933−928 cm^{-1} to the stretching of 3,6-anhydro-D-galactose.[33] Figure 10a depicts a comparison of the spectra of the pure V_{B2}, pure KCG, and a KCG-V_{B2} mixture at pH 1.2. The disappearance of the peak at 1380−1355 cm^{-1} and the sharp peak that appeared at 1240 cm^{-1} indicated that an electrostatic reaction might have taken place between the sulfate group and the cationic isoalloxazine of riboflavin.[32] The modification of the peak at 1126 cm^{-1} and the enlargement of the peaks at 1080−1010 cm^{-1} were indicative of effect of hydrogen bonding, and the modification of the peak at 928 cm^{-1} was also related to hydrogen bonding. These hydrogen bonds might have been between the glycosidic bond, 3,6-anhydro-D-galactose, and the ribitol of riboflavin. The proposed binding mechanism of KCG-V_{B2} is shown in Figure 11a. At pH 7.4, the enlargement of the peaks at 1270−1230 cm^{-1} and 1080−1010 cm^{-1} indicates that the ester sulfate group and glycosidic linkage might form hydrogen bonds with the ribitol of riboflavin. This binding mechanism is shown in Figure 11b. Based upon the above observation, the local molecular microstructure of KCG, consisting of the ester sulfate group, a glycosidic bond, and 3,6-anhydro-D-galactose, exhibited a specific adsorption of V_{B2}. This was why KCG could retard the release of V_{B2} (Figure 9b and d).

Figure 12 (left) shows CLSM micrographs depicting the gradual degradation of the typical WPsE film (WPI−KCG) and the release of oil from the film in pancreatin over time. During the initial stage (0.5 h), the film surface was gradually eroded by the enzyme and began to release the oil. Over 1−3 h, the film microstructure became damaged, and the oil embedded in the film was released. After 6 h, the film had dissociated into pieces, and the vitamins had been released into the water medium.

In a word, using the W/O/W double emulsion method, a WPsE film containing both the liposoluble and water-soluble vitamins was prepared under thermodynamically incompatible conditions. Different polysaccharides exhibited different synergistic effects with whey protein, producing different results with respect to the controlled release properties of the vitamins. The polysaccharide with the lowest charge was GA. It showed a strong emulsifying ability and exerted better control over the release of the liposoluble vitamin than more highly charged polysaccharides, such as KCG. These polysaccharides could be used to control the polar water-soluble vitamin. The simulated gastrointestinal test indicated that each investigated WPsE system had its own enteric release characteristics. This understanding was summarized in Figure 12 (right). Thus, this work indicates that a rational understanding of the functionalities of these common and safe materials will provide many possibilities for improving the application in cosmetic, pharmaceutical and food industries. It is anticipated that more effective formulations will be developed.

■ ASSOCIATED CONTENT

Supporting Information

Additional information as noted in the text. This material is available free of charge via the Internet at http://pubs.acs.org.

■ AUTHOR INFORMATION

Corresponding Author

*Phone: + 86-10-6273-7761. Fax: + 86-10-6273-6489. E-mail: xiaojing.leng@gmail.com.

Author Contributions

†F.L. and Y.J. contributed equally to this work.

Notes

The authors declare no competing financial interest.

■ ACKNOWLEDGMENTS

This research was supported by the National Natural Science Foundation of China (NSFC) (No. 31171771) and National Science and Technology Support Program (2011BAD23B04). Professor Liping Liang (China Agriculture University, Beijing, China) and professor Yunjie Yan (Beijing National Center for Microscopy, Tsinghua University, Beijing, China) were acknowledged for their technical advices.

■ REFERENCES

(1) Jiménez, A.; Fabra, M. J.; Talens, P.; Chiralt, A. Edible and biodegradable starch films: A Review. *Food Bioprocess Technol.* **2012**, 1−19.

(2) Valencia-Chamorro, S. A.; Palou, L.; Delŕio, M. A.; Pérez-Gago, M. B. Antimicrobial edible films and coatings for fresh and minimally processed fruits and vegetables: A review. *Crit. Rev. Food Sci. Nutr.* **2011**, *51*, 872−900.

(3) Aider, M. Chitosan application for active bio-based films production and potential in the food industry: Review. *LWT-Food Sci. Technol.* **2010**, *43*, 837−842.

(4) Vieira, M. G. A.; da Silva, M. A.; dos Santos, L. O.; Beppu, M. M. Natural-based plasticizers and biopolymer films: A review. *Eur. Polym. J.* **2010**, *47*, 254−263.

(5) Lewinski, N.; Colvin, V.; Drezek, R. Cytotoxicity of nanoparticles. *Small* **2008**, *4*, 26−49.

(6) Morillon, V.; Debeaufort, F.; Blond, G.; Capelle, M.; Voilley, A. Factors affecting the moisture permeability of lipid-based edible films: A review. *Crit. Rev. Food Sci. Nutr.* **2002**, *42*, 67−89.

(7) Wang, L.; Liu, L.; Holmes, J.; Huang, J.; Kerry, J. F.; Kerry, J. P. Effect of pH and addition of corn oil on the properties of whey protein isolate-based films using response surface methodology. *Int. J. Food Sci. Technol.* **2008**, *43*, 787−796.

(8) Weiss, J.; Takhistov, P.; McClements, D. J. Functional materials in food nanotechnology. *J. Food Sci.* **2006**, *71*, R107−R116.

(9) Li, Y.; Jiang, Y.; Liu, F.; Ren, F.; Zhao, G.; Leng, X. Fabrication and characterization of TiO_2whey protein isolate nanocomposite film. *Food Hydrocolloids* **2011**, *25*, 1098−1104.

(10) Dickinson, E. Double emulsions stabilized by food biopolymers. *Food Biophys.* **2011**, *6*, 1−11.

(11) Benichou, A.; Aserin, A.; Garti, N. Double emulsions stabilized with hybrids of natural polymers for entrapment and slow release of active matters. *Adv. Colloid Interface Sci.* **2004**, *108*, 29−41.

(12) Fechner, A.; Knoth, A.; Scherze, I.; Muschiolik, G. Stability and release properties of double-emulsions stabilised by caseinate-dextran conjugates. *Food Hydrocolloids* **2007**, *21*, 943−952.

(13) Wang, H.; Zhao, Y.; Wu, Y.; Hu, Y.-l.; Nan, K.; Nie, G.; Chen, H. Enhanced anti-tumor efficacy by co-delivery of doxorubicin and paclitaxel with amphiphilic methoxy PEG-PLGA copolymer nanoparticles. *Biomaterials* **2011**, *32*, 8281−8290.

(14) Salmieri, S.; Lacroix, M. Physicochemical properties of alginate/polycaprolactone-based films containing essential oils. *J. Agric. Food. Chem.* **2006**, *54*, 10205−10214.

(15) Murillo-Martínez, M. M.; Pedroza-Islas, R.; Lobato-Calleros, C.; Martínez-Ferez, A.; Vernon-Carter, E. J. Designing $W_1/O/W_2$ double emulsions stabilized by protein−polysaccharide complexes for producing edible films: Rheological, mechanical and water vapour properties. *Food Hydrocolloids* **2011**, *25*, 577−585.
(16) Chapel, J.-P.; Berret, J.-F. Versatile electrostatic assembly of nanoparticles and polyelectrolytes: Coating, clustering and layer-by-layer processes. *Curr. Opin. Colloid Interface Sci.* **2012**, *17*, 97−105.
(17) Song, Y. B.; Lee, J. S.; Lee, H. G. α-Tocopherol-loaded Ca-pectinate microcapsules: Optimization, *in vitro* release, and bioavailability. *Colloids Surf. B* **2009**, *73*, 394−398.
(18) Chen, L.; Subirade, M. Alginate-whey protein granular microspheres as oral delivery vehicles for bioactive compounds. *Biomaterials* **2006**, *27*, 4646−4654.
(19) Banerjee, R.; Chen, H. Functional properties of edible films using whey protein concentrate. *J. Dairy Sci.* **1995**, *78*, 1673−1683.
(20) Lefevre, T.; Subirade, M. Molecular differences in the formation and structure of fine-stranded and particulate β-lactoglobulin gels. *Biopolymers* **2000**, *54*, 578−586.
(21) Li, B.; Jiang, Y.; Liu, F.; Chai, Z.; Li, Y.; Leng, X. Synergistic effects of whey protein-polysaccharide complexes on the controlled release of lipid-soluble and water-soluble vitamins in $W_1/O/W_2$ double emulsion systems. *Int. J. Food Sci. Technol.* **2012**, *47*, 248−254.
(22) Messina, P. V.; Verdinelli, V.; Schulz, P. C. Sodium dioctylphosphinate emulsifier properties. *Colloid Polym. Sci.* **2006**, *285*, 251−261.
(23) Jiang, Y.; Li, Y.; Chai, Z.; Leng, X. Study of the physical properties of whey protein isolate and gelatin composite films. *J. Agric. Food. Chem.* **2010**, *58*, 5100−5108.
(24) Rhim, J. W.; Hong, S. I.; Ha, C. S. Tensile, water vapor barrier and antimicrobial properties of PLA/nanoclay composite films. *LWT—Food Sci. Technol.* **2009**, *42*, 612−617.
(25) Heilig, A.; Göggerle, A.; Hinrichs, J. Multiphase visualisation of fat containing [beta]-lactoglobulin-[kappa]-carrageenan gels by confocal scanning laser microscopy, using a novel dye, V03−01136, for fat staining. *LWT—Food Sci. Technol.* **2009**, *42*, 646−653.
(26) Flores, S.; Conte, A.; Campos, C.; Gerschenson, L.; Del Nobile, M. Mass transport properties of tapioca-based active edible films. *J. Food Eng.* **2007**, *81*, 580−586.
(27) Ghazanfari, A.; Emami, S.; Tabil, L.; Panigrahi, S. Thin-layer drying of flax fiber: I. Analysis of modeling using Fick's second law of diffusion. *Drying Technol.* **2006**, *24*, 1631−1635.
(28) Tuinier, R.; Dhont, J.; De Kruif, C. Depletion-induced phase separation of aggregated whey protein colloids by an exocellular polysaccharide. *Langmuir* **2000**, *16*, 1497−1507.
(29) Leng, X.; Turgeon, S. Study of the shear effects on the mixture of whey protein/polysaccharides—2: Application of flow models in the study of the shear effects on WPI/polysaccharide system. *Food Hydrocolloids* **2007**, *21*, 1014−1021.
(30) Ercelebi, E. A.; Ibanoğlu, E. Influence of hydrocolloids on phase separation and emulsion properties of whey protein isolate. *J. Food Eng.* **2007**, *80*, 454−459.
(31) Li, B.; Jiang, Y.; Liu, F.; Chai, Z.; Li, Y.; Leng, X., Study of the encapsulation efficiency and controlled release property of whey protein isolate--polysaccharide complexes in $W_1/O/W_2$ double emulsions. *Int. J. Food Eng.* **2011**, *7*.
(32) Drössler, P.; Holzer, W.; Penzkofer, A.; Hegemann, P. pH dependence of the absorption and emission behaviour of riboflavin in aqueous solution. *Chem. Phys.* **2002**, *282*, 429−439.
(33) Şen, M.; Erboz, E. N. Determination of critical gelation conditions of κ-carrageenan by viscosimetric and FT-IR analyses. *Food Res. Int.* **2010**, *43*, 1361−1364.